Geological Quarterly, 2007, **51** (1): 1–16

Hydrodynamic modelling, environmental tracers and hydrochemistry of a confined sandy aquifer (Kędzierzyn-Głubczyce Subtrough, SW Poland)

Stanisław WITCZAK, Tadeusz SZKLARCZYK, Ewa KMIECIK, Jadwiga SZCZEPAŃSKA, Andrzej ZUBER, Kazimierz RÓŻAŃSKI and Marek DULIŃSKI

Witczak S., Szklarczyk T., Kmiecik E., Szczepańska J., Zuber A., Różański K. and Duliński M. (2007) — Hydrodynamic modelling, environmental tracers and hydrochemistry of a confined sandy aquifer (Kędzierzyn-Głubczyce Subtrough, SW Poland). Geol. Quart., **51** (1): 1–16. Warszawa.

Sarmatian sands and buried Pleistocene valleys of the Kędzierzyn-Głubczyce Subtrough represent one of the main aquifers in southern Poland (MGWB-332 — Major Ground Water Basin). This aquifer is intensively exploited, supplying tap water for the human population and for industry in the whole area; but, being confined, it has no influence on the ground water ecosystems. Two Ground Water Bodies (GWB-128 and GWB-129), introduced by administrative decisions according to EU Directives, approximately cover the area of MGWB-332. The present study is related to the eastern part, the Sarmatian and buried valleys sands of MGWB-332, i.e. to the most important part of the multi-aquifer GWB-129 which in profile consists of Holocene and Pleistocene sands, confined Sarmatian and Pleistocene buried valley sands, and Badenian sands. The presence and influence of deeper permeable formations is not addressed. The Sarmatian and Badenian aquifers are recharged and drained mainly by vertical seepages. Hydrodynamic modelling of the whole Kędzierzyn-Głubczyce Subthrough and tracer data indicate modern ages at the outcrops of the Sarmatian under the Pleistocene deposits and mid to early Holocene ages close to the Odra River valley. Waters are of the HCO_3-Ca type, changing at the centre of the Sarmatian to the SO_4-Ca type due to the contribution of ascending sulphate water from the Badenian strata, whereas water in the buried Quaternary valley is of the HCO_3-Na type, which means no significant contribution of ascending waters. Polluted modern waters occur only at the northwestern boundary in the area of the hydrogeological window. The quality of waters and their hydrochemistry result from water-rock interactions and seepage exchanges with overlying and underlying aquifers belonging to the same GWB. Natural distributions of most major, minor and trace constituents are very wide, exemplifying difficulties in defining the quality of water in a unique way for the whole aquifer and particularly for the investigated multi-aquifer GWB.

Stanisław Witczak, Tadeusz Szklarczyk, Ewa Kmiecik and Jadwiga Szczepańska, Faculty of Geology, Geophysics and Environmental Protection, AGH University of Science and Technology, Al. Mickiewicza 30, PL-30-059 Kraków, Poland; Andrzej Zuber, Polish Geological Institute, Carpathian Branch, Skrzatów 1, PL-31-560 Kraków, Poland; Kazimierz Różański and Marek Duliński, Faculty of Physics and Applied Computer Science, AGH University of Science and Technology, Al. Mickiewicza 30, PL-30-059 Kraków, Poland (received: December 15, 2006; accepted: March 13, 2006).

Key words: confined aquifers, hydrodynamic modelling, environmental tracers, hydrochemistry, water quality.

INTRODUCTION

European Union Directives (1998, 2000 and 2006) are aimed at the proper management of ground water systems, including preservation of ground water resources, which are often of good quality, for future generations. The EU Directives introduce the concept of a Ground Water Body (GWB), which means a distinct volume of ground water within an aquifer or aquifers, which has influence on human receptors and ground water dependent ecosystems. That definition is not precise, and requires lengthy description of factors which should be considered in the selection of GWB boundaries. As a consequence, the boundaries of GWBs in Poland are distantly related to the boundaries of major aquifers investigated earlier under national projects, though these were introduced by administrative regulations based on the work of experts from the Polish Geological Institute (Herbich *et al*., 2005).

To reach the aims stated in the Directives, one necessarily has to determine the natural or quasi-natural (baseline) quality of water defined by Natural Background Levels (NBL values) of water constituents. The quality of water depends on timescales of water-rock interactions and can be changed when mixed with or replaced by water of poorer quality, due to pollution, or better quality, due to remediation actions and enhanced recharge.

The present work contains earlier results obtained in the framework of the BASELINE Project (Edmunds and Shand, 2007) and preliminary results obtained within the ongoing

BRIDGE Project (http://www.wfd.bridge.net) for the multi-aquifer GWB-129. The BASELINE Project was aimed at obtaining typical NBL values whereas the BRIDGE Project is aimed at obtaining the basic material for the development of a proper methodology for the investigations of groundwater systems in accordance with EU Directives.

The Sarmatian sands and buried Pleistocene valleys of the Kędzierzyn-Głubczyce Subtrough, south-west Poland, form the main parts of GWB-129 and GWB-128, and belong to the category of the Main Ground Water Basins in Poland (MGWB-332), which were precisely defined by their hydraulic, output and quality parameters (Kleczkowski *et al*., 1990). The investigated GWB-129 consists of three aquifers of the following importance: Sarmatian and buried Pleistocene valley sands confined by Sarmatian clays and silts, unconfined Pleistocene and Holocene sands, and Badenian sands separated from the overlying and underlying formations by semi-permeable Badenian and Carpathian deposits. The contribution of permeable Triassic carbonates to the water balance of GWB-129 is negligible. The flow model covers the areas of GWB-129, GWB-128 and small parts of two other GWBs (Fig. 1), whereas the hydrochemical and tracer data are mainly related to the Sarmatian deposits of GWB-129, and were described in part by Duliński *et al*. (2002) and Szczepańska and Kmiecik (2005).

METHODS

The flow and transport modelling was performed with the aid of the MODFLOW (McDonald and Harbaugh, 1988), MODPATH (Pollock, 1988) and MT3D (Zheng and Wang, 1999) packages incorporated in Visual-MODFLOW (Guiger and Franz, 2003). The finite-difference grid for the flow and transport calculations consisted of 8 layers with 20 760 blocks of 500 × 500 m^2 (173 lines and 120 columns). As the model re-

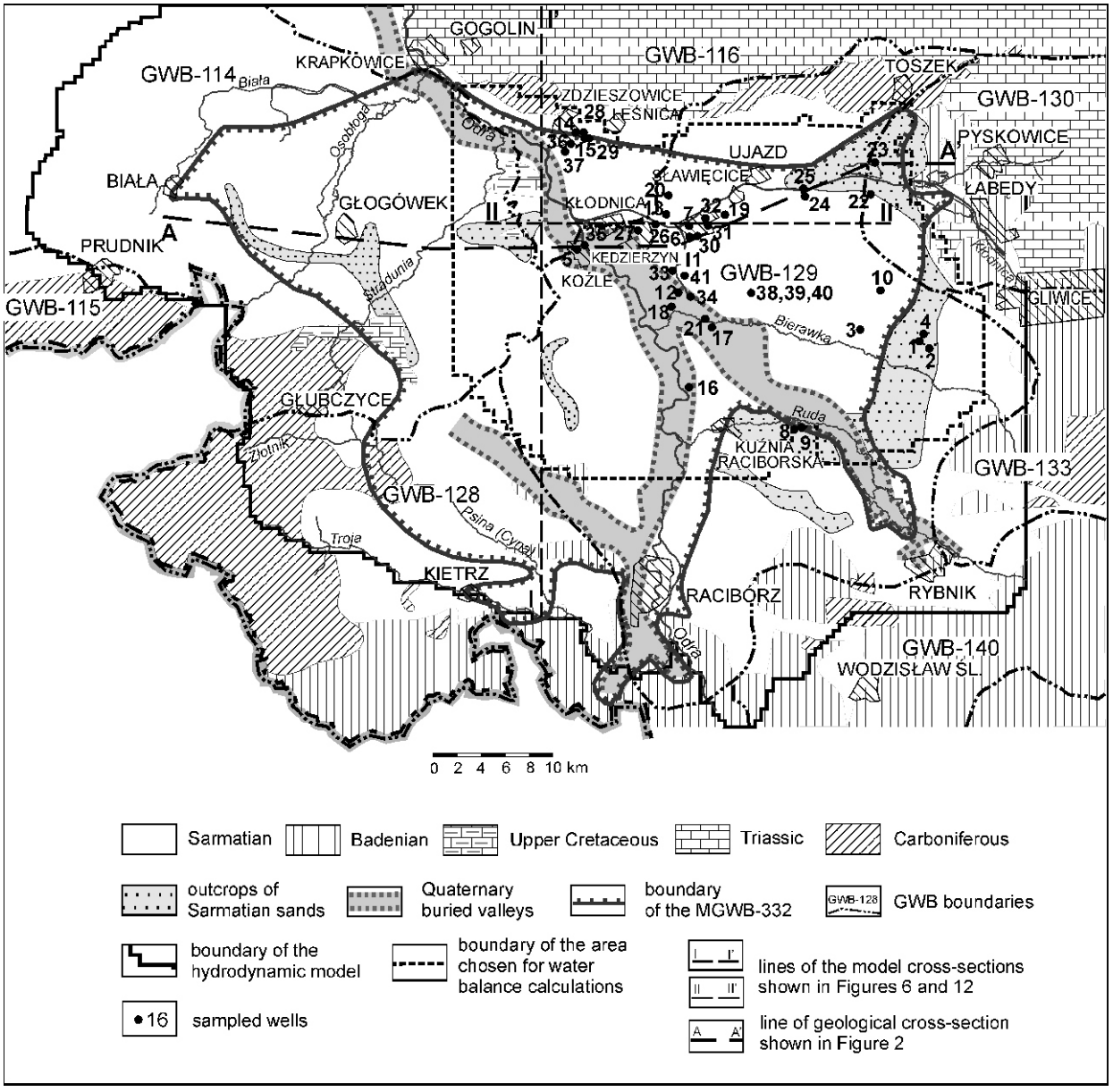

Fig. 1. Geological map of the Głubczyce-Kędzierzyn Subtrough (without Quaternary cover)

quires continuity of all layers, for the areas without a given layer its model thickness was assumed to be 1 m with the hydraulic conductivity of the layer from which that 1 m was subtracted. The MODFLOW River Package was used to simulate the exchange of water between aquifers and surface water with head-dependent seepage interaction.

The entire field procedures of hydrochemical sampling were similar to those described by Salminen (2005). Unfiltered water was placed into 500 ml polyethylene-bottles for major anion analysis, filtered water was acidified by HNO_3 to pH < 2 and taken to new hardened polyethylene 100 ml bottles for ICP-MS and ICP-AES and other routine analysis methods for major, minor and trace components. Filtered water was also taken to 100 ml umber-glass bottles for DOC analysis. For pH and Eh field determinations, two laboratory-calibrated instruments measured the outflowing pumped water online in a flow-through cell until stable readings were reached. If the readings of both instruments differed, the mean value was taken. Alkalinity was measured in the field by the titration method. Uncertainties of chemical analyses are related to the last one or two digits of the values reported.

Only selected wells were sampled for analyses of environmental tracers. Tritium and ^{14}C were measured by standard techniques (electrolytic enrichment followed by liquid scintillation spectrometry for tritium, and benzene synthesis followed by liquid scintillation spectrometry for ^{14}C). Stable isotope composition ($\delta^{18}O$, $\delta^{2}H$ and $\delta^{13}C$) was determined by isotope ratio mass spectrometry and expressed versus V-SMOW and V-PDB standards (Coplen, 1996). Sulphur hexafluoride (SF_6) was measured by electron-capture gas chromatography with the headspace extraction technique (Śliwka *et al*., 2004). However, as SF_6 concentrations significantly depend on the air excess entrapped in the recharge areas (Busenberg and Plummer, 2000; Zuber *et al*., 2005), which was not controlled, they were used only to confirm modern ages indicated by tritium contents. Standard uncertainties of ^{14}C, $\delta^{18}O$, $\delta^{2}H$, $\delta^{13}C$ and SF_6 analyses were 1.0 pmc, 0.1, 1, 0.1‰ and 0.01–0.02 fmol/L, respectively. Uncertainties of tritium were from 0.5 T.U. for the lowest contents to about 1 T.U. for the highest contents.

HYDROGEOLOGY

The study area of about 3675 km^2 is situated in southwestern Poland with the upper transboundary Odra River flowing from the SSE to NNW through the centre of the basin consisting of the Głubczyce Upland (235–260 m a.s.l.) and the Racibórz valley (180–200 m a.s.l.), with the mean annual precipitation rate and temperature around 770 mm and 8°C, respectively. The geological map of the structure, called the Głubczyce-Kędzierzyn Subtrough, is shown in Figure 1, without the Quaternary cover. The geological cross-section and the stratigraphic profile are shown in Figures 2 and 3, respectively.

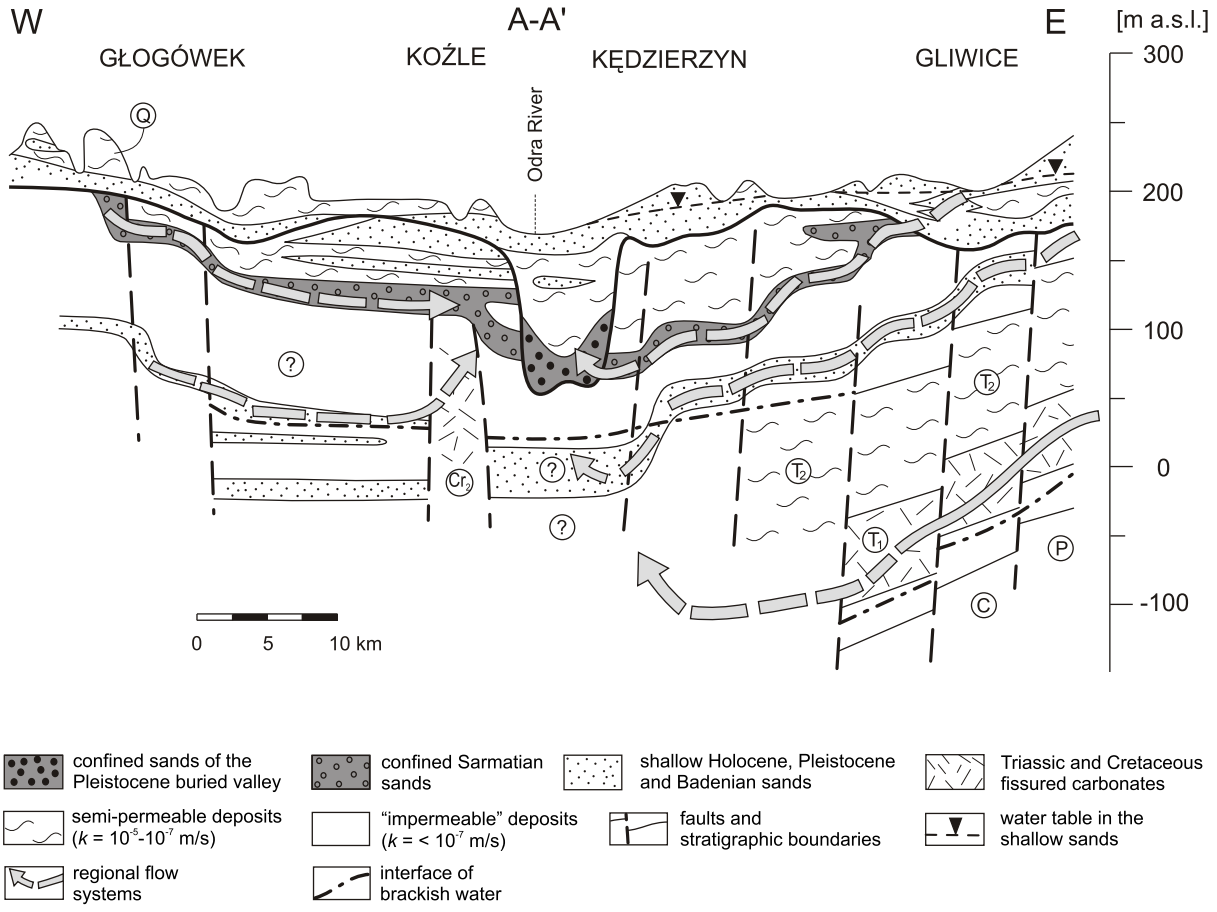

Fig. 2. Simplified geological cross-section of the study area (the main aquifer is shaded)

Q — Quaternary, Cr_2 — Upper Cretaceous, T_2 — Middle Triassic, T_1 — Lower Triassic, P — Permian, C — Carboniferous

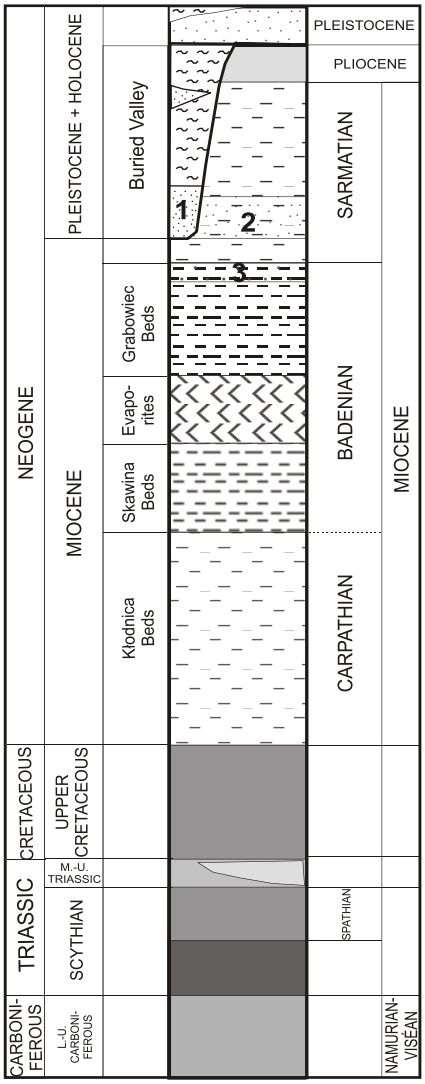

Fig. 3. Stratigraphic profile

1 — sands of Pleistocene buried valley,
2 — Sarmatian sands, 3 — Badenian sands

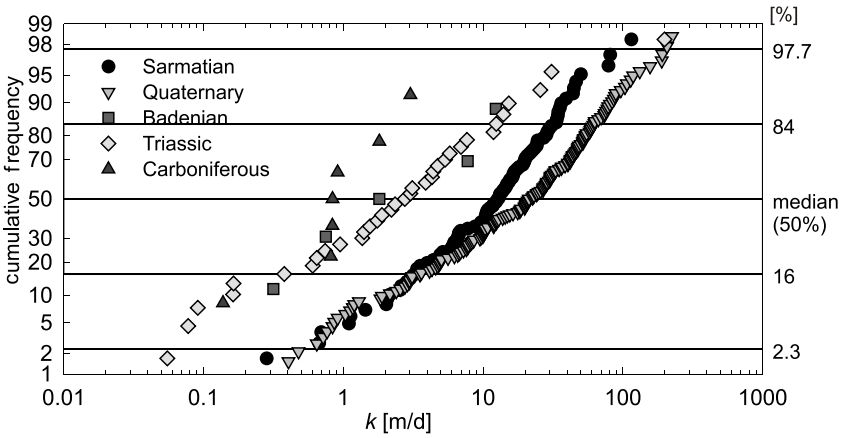

Fig. 4. Cumulative distributions of the hydraulic conductivity

Unconfined Quaternary sands and gravels 5–30 m thick represent the shallow aquifer whereas Pleistocene deposits are up to 120 m thick in the buried Odra River valley. The buried valleys at grater depths are filled with sands and gravels. These are separated from the upper permeable layers by glacial tills in the central part of the area whereas in the south-east glacial tills occur only locally. The Sarmatian aquifer is formed of medium and coarse sands with gravels and traces of brown coal in the central part where it is hydraulically connected with the Pleistocene buried valleys. That aquifer is separated from the Pleistocene deposits by semi-permeable Sarmatian clays and silts, and in very small areas by Pliocene silts. The Sarmatian aquifer is 15 to 30 m thick, reaching 70–100 m within the central part of the area whereas near the outcrops this unit lies at only 30 to 40 m below the ground level. Deeper formations are poorly known but Badenian clays separate the Sarmatian sands from fine Badenian sands, which are underlain in turn by semi-permeable Badenian and Carpathian deposits (claystones and madstones of Kłodnica Beds). Cretaceous carbonates locally occur below the Miocene deposits mainly to the west of the Odra River, Triassic carbonates extend across the whole area whereas Carboniferous shales and sandstones rocks have been recognized only in some areas at the boundaries of the basin (see Fig. 1). More detailed descriptions of the geology can be found in a number of papers (e.g. in Kleczkowski, 1966; Alexandrowicz and Kleczkowski, 1968, 1970; Kotlicka, 1975, 1978, 1981).

The cumulative distributions of the hydraulic conductivities of the main water-bearing formations are shown in Figure 4. The geometric mean of the hydraulic conductivity of the Sarmatian sands is 12 m/d (1.2×10^{-4} m/s) and for the Badenian sands is 1.7 m/d (0.2×10^{-4} m/s). Holocene and Pleistocene aquifers have higher hydraulic conductivity than the Sarmatian aquifers, whereas the Triassic aquifer has similar values to those of the Badenian one.

Regional flow is to the Odra River, which is the south-west boundary of the area chosen for the hydrochemical and tracer study seen in Figure 1 from the positions of sampled wells. The shallow Pleistocene aquifer is recharged directly by precipitation and drained directly by the Odra River and its tributaries. The Sarmatian aquifer is recharged indirectly from the Pleistocene deposits at the outcrops of the Sarmatian sands, by downward seepage and through the erosion window at the northern boundary (wells 28 and 29). At the northern boundary the recharge is mainly by lateral flow from Triassic and Carboniferous formations, and in the central part by upward seepage from Badenian sands. The Badenian sands are recharged in the outcrops from the Quaternary deposits and by seepage from the Sarmatian sands. The Pleistocene buried valleys are recharged by lateral flow from unconfined upstream areas and from the Sarmatian deposits. The drainage of the Sarmatian and deeper formations is by subsequent upward seepage to the shallow Pleistocene deposits, which takes place mainly along the Odra River valley.

The natural flow pattern has changed due to intensive withdrawal from the Sarmatian aquifer by wells with depths of 80–120 m, situated mainly in the central part of the area, close to the buried Quaternary valley, which also supplies water. Water withdrawal began around 1920, but intensive exploitation

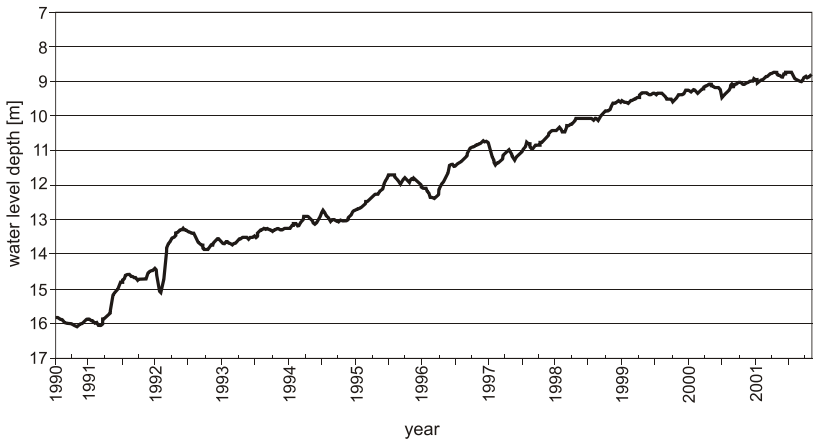

Fig. 5. Recovery of water level in the state monitoring well in Stara Kuźnia (no. 39)

started in 1950, reaching a maximum in the period 1975–1990. Due to political and economical changes, the consumption of water dropped around 1990 from *ca*. 120 000 to *ca*. 60 000 m^3/day, which resulted in the recovery of the water table observed in the state monitoring well no. 39 (Fig. 5).

ENVIRONMENTAL TRACERS

Environmental tracer data are presented in Table 1 together with ages estimated from tritium and ^{14}C contents. With two exceptions discussed further, $\delta^{18}O$ and $\delta^{2}H$ values agree with those indicated on maps of the isotopic composition of waters recharged in that region of Poland in the Holocene (d'Obyrn *et al*., 1997). The presence of modern waters in the recharge area in the east and at the northern boundary is indicated by measurable tritium contents in some wells. Quantitative age estimations for these modern waters can be obtained only as a rough approximation due to low numbers of tritium determinations. The interpretation was performed with the aid of the FLOWPC program (Małoszewski and Zuber, 1996). Double- or triple-parameter models are usually most adequate for exploitation wells which never have flow lines with infinitively short travel times required by the exponential model (EM), but their use is little justified when short series of data are available as is the case in this study. Therefore, for each sampled well, the extreme single-parameter models, i.e. the piston flow (PFM) and exponential (EM) model, were used to obtain estimates of bracket age values. However, for well no. 4, with an increasing tritium content, the dispersion model (DM) had to be used instead of the EM because in such a case the latter is not applicable.

The youngest water was found in well no. 2, which was confirmed by the highest SF_6 content of 1.52 to 1.97 fmol/L. Tritium and SF_6 contents (about 0.10–0.16 fmol/L) considered together indicate that wells no. 15 and 28 exploit similar water as does well no. 2, though somewhat older. A sharp change in tritium content observed in well 15 is not interpretable by any model. For that well, changes in withdrawal rates most probably caused a sharp change in the age of exploited water, which is not surprising as that well is situated in the area of the hydrogeological window. Wells 1, 3, 14 and 22 undoubtedly contain pre-bomb era waters with admixtures of quite young modern waters because their tritium data cannot be interpreted by the PFM without an assumption of a tritium-free component. In the case of decreasing tritium contents (no. 1, 3 and 14), the tritium age cannot be related to initial stage of the bomb era when the atmospheric contents of that tracer were rising, i.e. the period of 1952–1962. The SF_6 contents in these four wells were in the range of 0.04–0.16 fmol/L, i.e. too high for the period of 1952–1962.

The apparent ^{14}C ages given in Table 1 were estimated by the piston flow approximation with a simple correction of the initial carbon content (e.g. see Clark and Fritz, 1997):

$$\textit{Apparent Age}\ [\text{ka}] \cong 8300 \times \ln[qC_o/{}^{14}\text{C}] \qquad [1]$$

where: C_o is the uncorrected initial ^{14}C content [100 pmc], ^{14}C — measured value, q — correction coefficient represented in the simplest form by:

$$q = \frac{\delta^{13}C_{DIC} - \delta^{13}C_{\text{CaCO}_3}}{\delta^{13}C_{soil} - \delta^{13}C_{\text{CaCO}_3}} \qquad [2]$$

where: $\delta^{13}C_{DIC}$ — measured value for total dissolved inorganic carbon (DIC), $\delta^{13}C_{soil}$ — assumed value of –25‰ for soil CO_2, $\delta^{13}C_{\text{CaCO}_3}$ — assumed value of 0‰ for "dead" carbon in solid material undergoing dissolution.

The correction expressed by Equation [2] and all other methods used to account for the influence of carbon hydrochemistry on ^{14}C dating are not regarded as very reliable. Much more reliable is the determination of age differences between two wells on the same flow line, which reads as follows:

$$\textit{Age difference}\ [\text{ka}] = 8300 \times \ln[p^{14}C_1/{}^{14}C_2] \qquad [3]$$

where: $^{14}C_1$ and $^{14}C_2$ are the radiocarbon contents in DIC at points 1 and 2, respectively, and $p = \delta^{13}C_{DIC_2}/\delta^{13}C_{DIC_1}$ is assumed to account for further contribution of dissolved dead carbonates.

For a number of samples containing significant tritium contents, the apparent ^{14}C ages are of the order of several thousand years whereas they should be modern (see Table 1). Such an effect can be explained by two hypotheses. First, that older tritium-free water mixes with modern water, and second, that initial ^{14}C content is much more reduced than calculated from Equation [1]. The effect of mixing is only evident for the sample taken from the shallow Pleistocene aquifer monitored by the state network (no. 38) where an early Holocene age is suggested by the low ^{14}C concentration (9.7 pmc), though the presence of modern water is indicated by the high tritium concentration (9.4 T.U.). Neither the tritium data nor the chemical data of waters from wells no. 2 and 4 indicate the possibility of significant mixing, whereas the tritium data of wells no. 1 and 3 suggest very wide age distributions, which means mixing of

Table 1

Tracer data and estimated ages of waters in the Sarmatian and buried Pleistocene valley (no. 1–37 and 39), shallow Pleistocene (no. 38) and Triassic (nos. 40 and 41)

No.	Date	^{18}O [‰]	^{2}H [‰]	^{14}C [pmc]	^{13}C [‰]	^{14}C age, app./diff. [10^3 years]	Tritium [T.U.]	Model	^{3}H age [years]
1	10.09.00 20.06.01	–9.4 –9.5	–65 –67	36.3 n.m.	–13.4 n.m.	3.3/modern	3.0 0.5 1.3 0.5	PFM EM	(1) 700
2	10.09.00 20.06.01	–9.9 –9.7	–68 –71	n.m. 38.8	n.m. –14.5	– 3.3/modern	13.0 0.5 11.4 0.5	PFM EM	4 8
3	10.09.00 20.06.01	–9.6 –9.7	–67 –69	39.1 n.m.	–14.2 n.m.	3.1/modern	5.9 0.5 5.4 0.5	PFM EM	(1) 245
4	05.09.00 20.06.01	–9.8 –9.8	–68 –70	39.1 n.m.	–14.3 n.m.	3.2/modern	3.7 0.5 5.2 0.5	PFM DM	47.5 4.5
6	04.09.00	–10.1	–71	16.4	–13.5	9.9/6.3	0.0 0.5		
7	04.09.00	–10.1	–71	15.3	–12.8	10.0/6.9	0.0 0.5		
11	06.09.00	–9.7	–68	25.1	–14.4	6.9/2.7	0.0 0.5		
12	06.09.00	–9.9	–69	20.4	–12.9	7.7/4.5	0.0 0.5		
13	08.09.00	–10.2	–72	15.2	–12.6	9.9/6.9	0.1 0.5		
14	06.09.00 27.06.01 18.07.01	–10.2 –10.3 –10.2	–71 –76 –73	47.8 n.m. n.m.	–13.1 n.m. n.m.	0.76/modern	2.4 0.5 2.3 0.5 1.7 0.5	PFM EM	(1) 650
15	06.09.00 27.06.01	–10.0 –10.1	–71 –72	68.3 n.m.	–16.0 n.m.	modern	23.3 1.1 12.6 0.7	PFM EM	(2)
16	19.05.82	–10.0	–71	n.m.	n.m.		0.0 1.5		
19	27.06.01	–10.1	–72	17.7	–12.6	8.7/5.7	0.0 0.5		
20	27.06.01	–10.3	–72	15.7	–12.6	9.7/6.7	0.1 0.5		
21		–10.0	–70				0.0 0.5		
22	10.07.01	–9.8	–69	n.m.	n.m.		4.4 0.5	PFM/EM	(1)/320
23	10.07.01	–9.9	–70	n.m.	n.m.		0.3 0.5		
24	03.07.01	–10.2	–72	17.4	–11.9	8.4/5.8	0.2 0.5		
28	18.07.01	–9.4	–69	n.m.	n.m.		13.8 0.8	PFM/EM	5/29
36	18.07.01	–10.1	–72	n.m.	n.m.		0.2 0.5		
37	18.07.01	–10.1	–73	n.m.	n.m.		0.0 0.5		
38	01.10.01	–10.0	–69	9.7	–18.9	mixed water	9.4 0.8		(3)
39	01.10.01	–9.4	–65	14.4	–14.5	11.6/7.4	0.0 0.5		
40	01.10.01	–10.6	–74	9.6	–21.4	18.2/10.7	1.8 0.6		
41	27.08.01	–10.7	–74	0.3	–9.0	40/36	0.0 0.5		

PFM — piston flow model, EM — exponential model, DM — dispersion model, n.m. — not measured; remarks to ^{3}H age: 1 — non-interpretable by PFM without assuming the presence of tritium-free water component (see text), 2 — non-interpretable by any model, 3 — mixed pre-bomb era water (low ^{14}C) with modern (high ^{3}H)

modern water containing tritium with tritium-free water. For wells in the recharge area, both mixing components can be regarded as being very young in terms of the ^{14}C method. Therefore, though the mixing hypothesis cannot be rejected, the second hypothesis is also acceptable because the apparent ^{14}C age of no. 39 suggests the possibility of recharge in pre-Holocene time, which is not confirmed by $\delta^{18}O$ and $\delta^{2}H$ values typical of Holocene waters. A careful inspection of the ^{14}C and $\delta^{13}C_{DIC}$ data of Table 1 suggests that 35 pmc and –14.5‰ can be accepted in a rough approximation as initial values for young

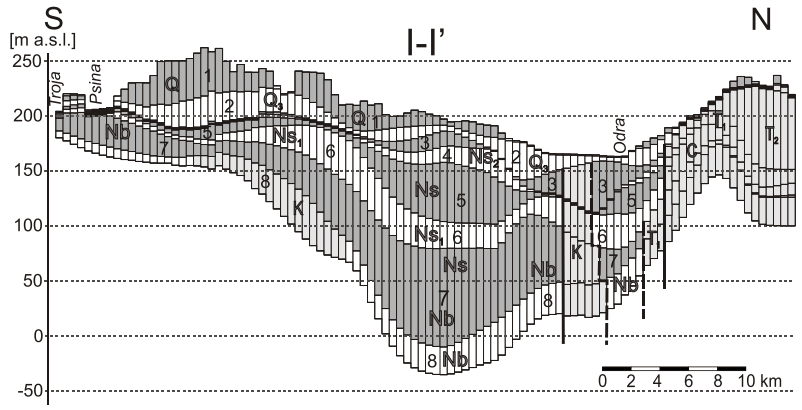

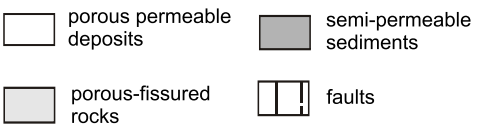

Fig. 6. Geological structure for the hydrodynamic modelling

Q_1, Q_2, Q_3 — Holocene and Pleistocene; Ns, Ns_1, Ns_2 — Sarmatian, Nb — Badenian, K — Upper Cretaceous, T_2 — Middle Triassic, T_1 — Lower Triassic, C — Carboniferous; 1–8 — layer number of the model

pre-bomb era waters in the recharge area. Then, the age difference between waters in the recharge area and those downstream can be expressed by Equation [4], which can be regarded as an approximation of Equation [3].

$$\textit{Age difference}\ [\text{ka}] \cong 8300 \times \ln[p35/^{14}C] \qquad [4]$$

where: $p = \delta^{13}C_{DIC}/(-14.5)$.

The ^{14}C age differences obtained from Equation [4] are given in Table 1 together with the apparent ages. Most probably, the real ^{14}C ages lie within the ranges given by these two quantities. For the system investigated, Equation [4] satisfies the extreme age values, i.e. modern ages observed in some waters in the Sarmatian and reasonable glacial ages in the Triassic aquifer expected from more negative $\delta^{18}O$ and $\delta^{2}H$ values observed in well no. 40 and 41. That correction removes also the inconsistency observed in well no. 39 where the apparent ^{14}C age is close to 12 ka whereas the isotopic composition of water indicates recharge under a Holocene climate. Therefore, Equation [4] can be regarded as the result of "calibration" of the observed extreme ^{14}C data to the known extreme ages. For well no. 40, where an unusual value of $\delta^{13}C_{DIC}$ was obtained (–21.4‰), the apparent age is in the range of the last glacial maximum (LGM) whereas the age difference of 10.7 ka is acceptable (p = 1.0 was assumed). A very old age obtained for water in the Triassic strata of well no. 41 is not surprising considering the glacial age of water in well no. 40 at a large upstream distance.

The ^{14}C ages given in Table 1 can be somewhat overestimated due to the losses of ^{14}C caused by diffusion. Namely, in confined aquifers of small thickness and large extents, the movement of any tracer can be delayed due to diffusion exchange either with confining formations as shown for ^{14}C by Sudicky and Frind (1981) or with impermeable interbeds as shown by Sanford (1997). According to the formula of Sudicky and Frind, due to a low thickness of the Sarmatian sands (15–30 m), that effect could be significant if the flow were only horizontal. However, the influence of diffusion exchange on age values is reduced in cases of advective gains and/or losses, i.e. when upward and downward seepages exist. As it is difficult to estimate all effects leading to the possible reduction of ^{14}C in the study area, the ^{14}C ages given in Table 1 should be regarded as upper estimates of real values.

NUMERICAL FLOW AND MIGRATION MODELLING

The whole modelled area of 5 500 km^2 is much larger than the area of the aquifers investigated (see Fig. 1). Data from more than 600 wells were used for the construction of the model, whereas the water levels from 268 wells were taken for the calibration (Szklarczyk *et al.*, 2004). An example of the model structure is given in Figure 6. The uppermost water-bearing layer (no. 2 in the model) is formed by near-surface Quaternary sands and gravels (Q_1). A deeper water-bearing layer (no. 4) consists of uppermost Sarmatian sands locally in contact with near-surface Quaternary deposits. The main Sarmatian sandy layer in hydraulic contact with deep Pleistocene buried valley includes layer no. 6. The Badenian layer has includes layer no. 8. The accepted structure of the model means that seepage from the Triassic strata was neglected whereas head and tracer data indicate the possibility of such seepage. The steady-state model was calibrated to the most complete withdrawal and water level data which were available for 1993. The comparison of calculated and observed heads is shown in Figure 7. Calculations were also performed for pseudo-natural steady-state conditions of the pre-exploitation era.

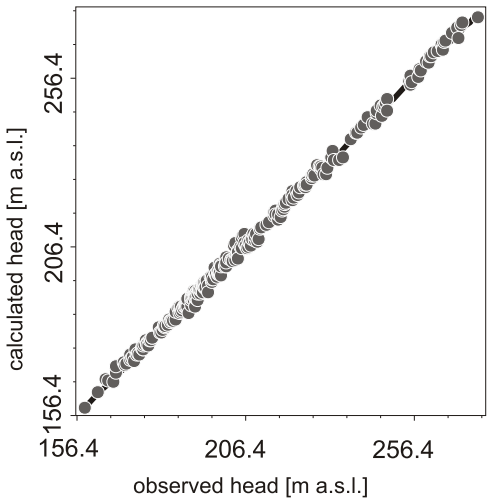

Fig. 7. Calculated and observed heads

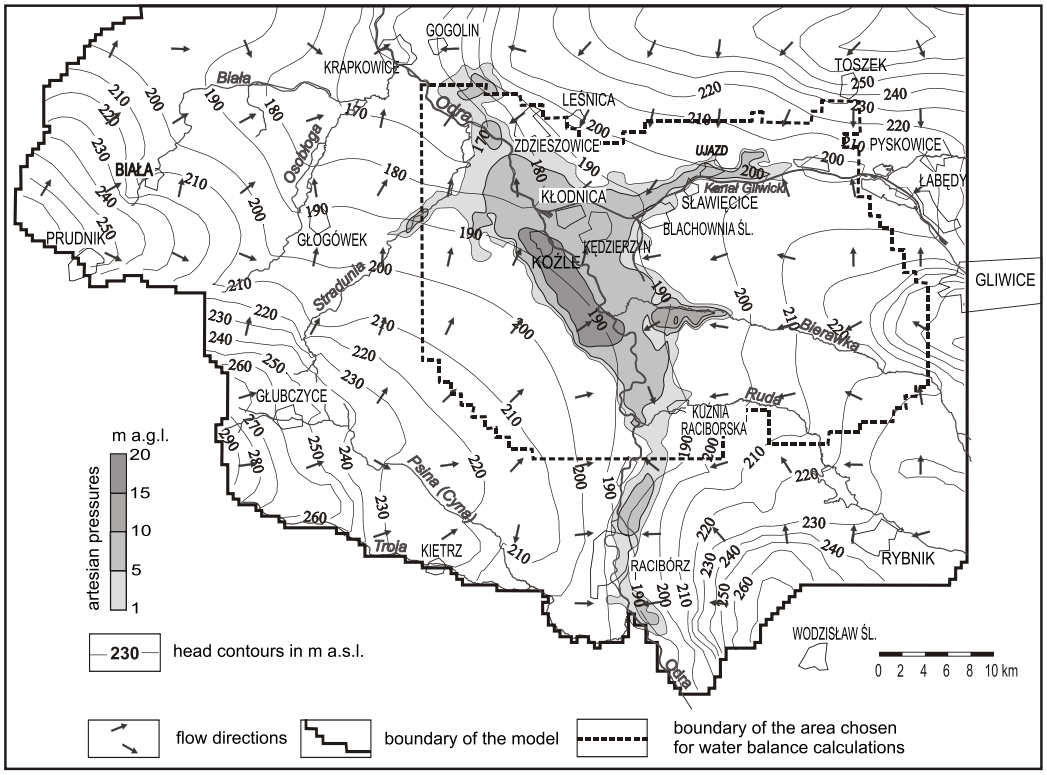

Fig. 8. Hydrodynamic map of layer no. 6 (Sarmatian deposits and Pleistocene buried valley) calculated for the pre-exploitation era

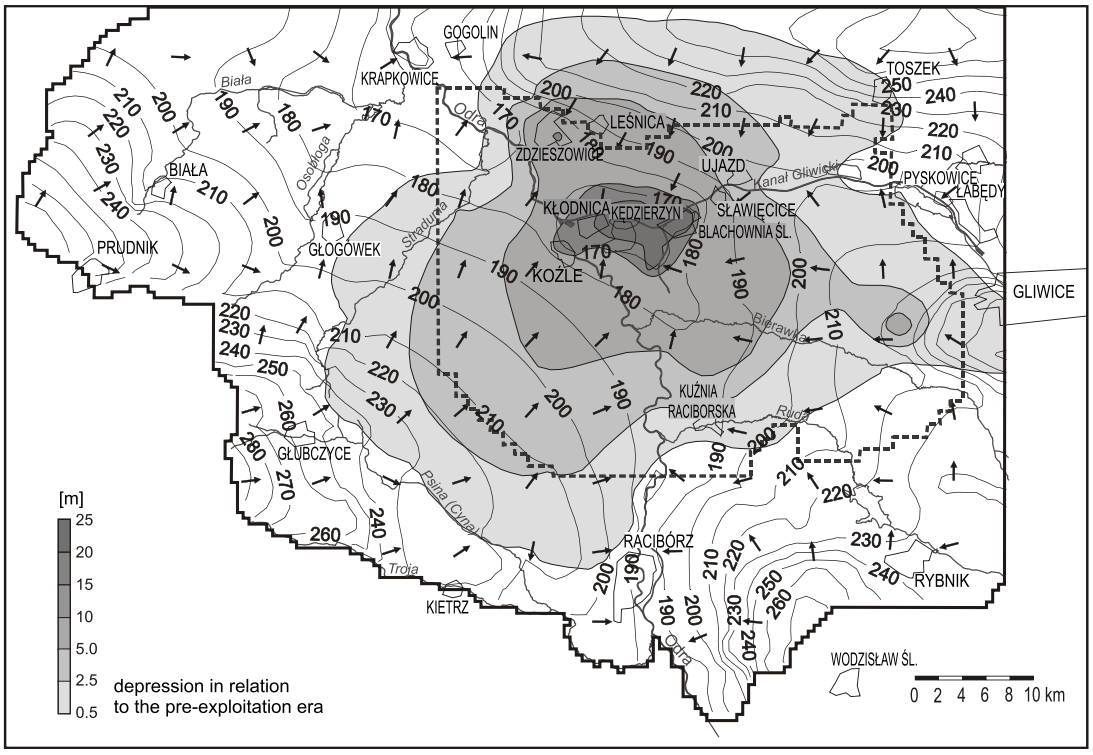

Fig. 9. Hydrodynamic map of layer no. 6 calculated for 1993

For other explanations see Figure 8

The head contours and artesian levels in the Sarmatian and connected Pleistocene deposits (layer 6) obtained for the pre-exploitation era are shown in Figure 8, whereas the depression levels in 1993 are shown in Figure 9. It can be seen from these two figures that, near the abstraction wells in the central area, the upward seepage from the Sarmatian to the Quaternary in pre-exploitation era changed to downward seepage, which resulted in increased downward seepage from the shallow Pleistocene aquifer. However, in most of the Odra River valley, artesian conditions still prevail in the Sarmatian. The artesian levels of the Badenian for 1993 are shown in Figure 10; they remained practically the same as those during the pre-exploitation era.

Water balance calculated for a smaller area (see Fig. 1) is shown in Figure 11. It can be seen that essentially only the Sarmatian aquifer is exploited and its intensive exploitation has no influence on the seepage rates between the Sarmatian and the Badenian. However, the downward seepage from the shallow Pleistocene to the Sarmatian deposits increased by *ca*. 14 000 m^3/d, and the upward seepage between these formations

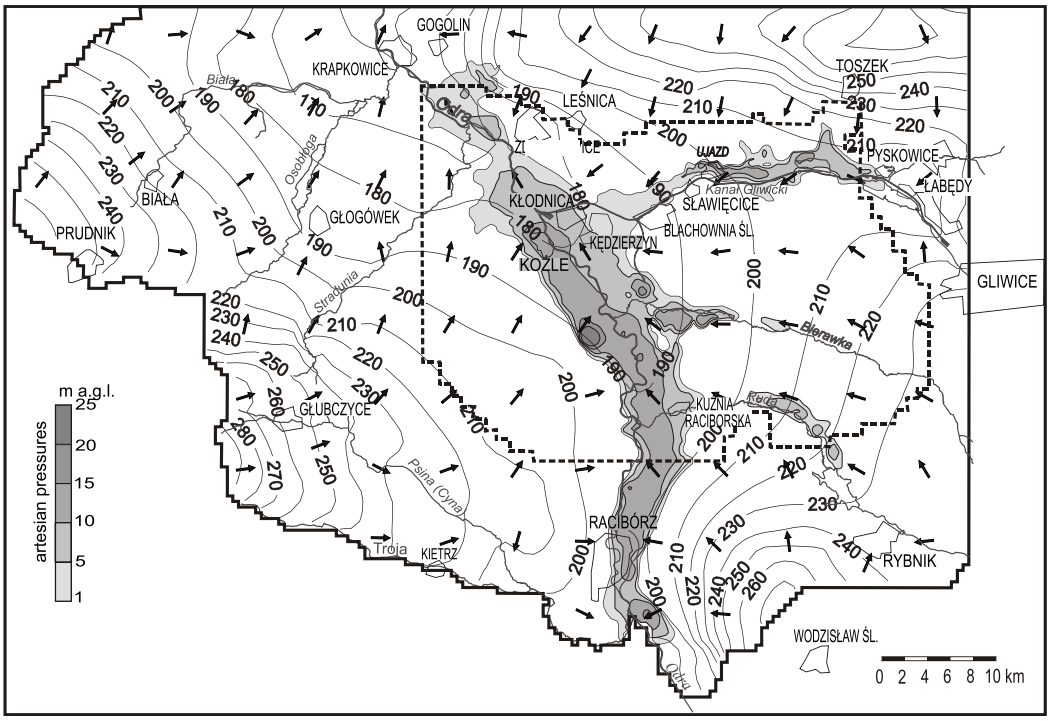

Fig. 10. Hydrodynamic map of layer no. 8 (Badenian) for 1993

For other explanations see Figure 8

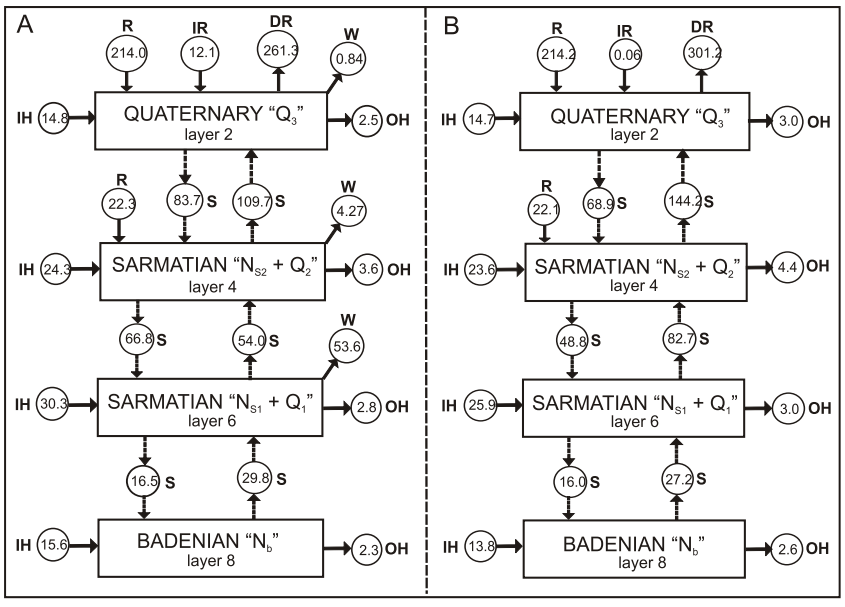

Fig. 11. Schematic presentation of water balance

A — calculations for 1993; B — pre-exploitation era; R — effective recharge from precipitation, IR — river infiltration, IH — horizontal inflow, S — seepages and inflow through hydrologic windows, DR — drainage to rivers, W — withdrawal, OH — horizontal outflow; notation of permeable layers as in Figure 6

decreased by *ca*. 44 000 m^3/d. The sum of these two figures gives a safe yield of *ca*. 60 000 m^3/d, which is two times lower than the maximum withdrawal rate in the period of 1975–1990.

Migration travel times along chosen flow lines calculated with the aid of MODPATH are shown in Figure 12 for a chosen cross-section. They are in a reasonable agreement with the ^{14}C data which indicated the dominant presence of early Holocene water in the central part of the Sarmatian aquifer. Intermediate ^{14}C ages calculated with the aid of Equation [3] are also qualitatively consistent with the results of modelling

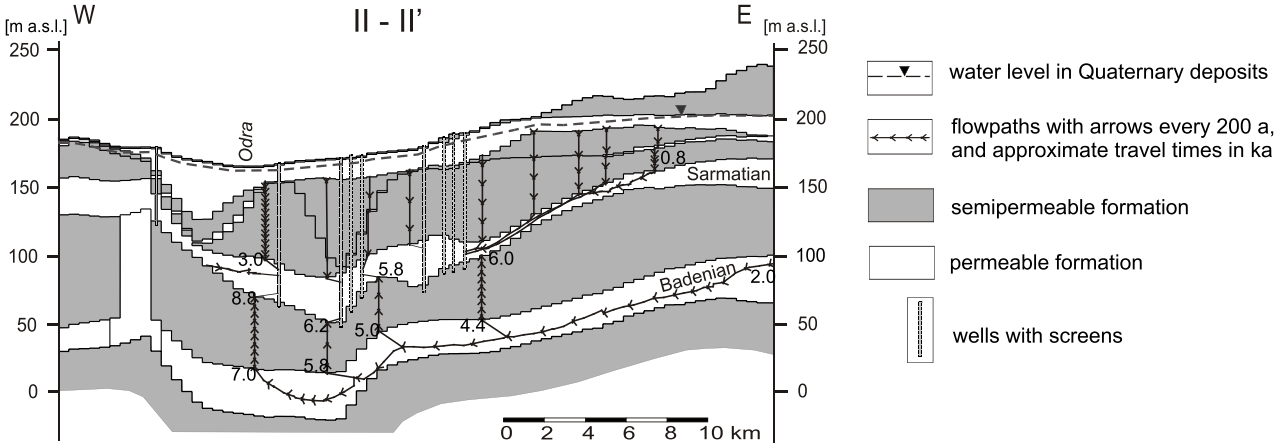

Fig. 12. An example of the model cross-section with travel times along chosen flow paths

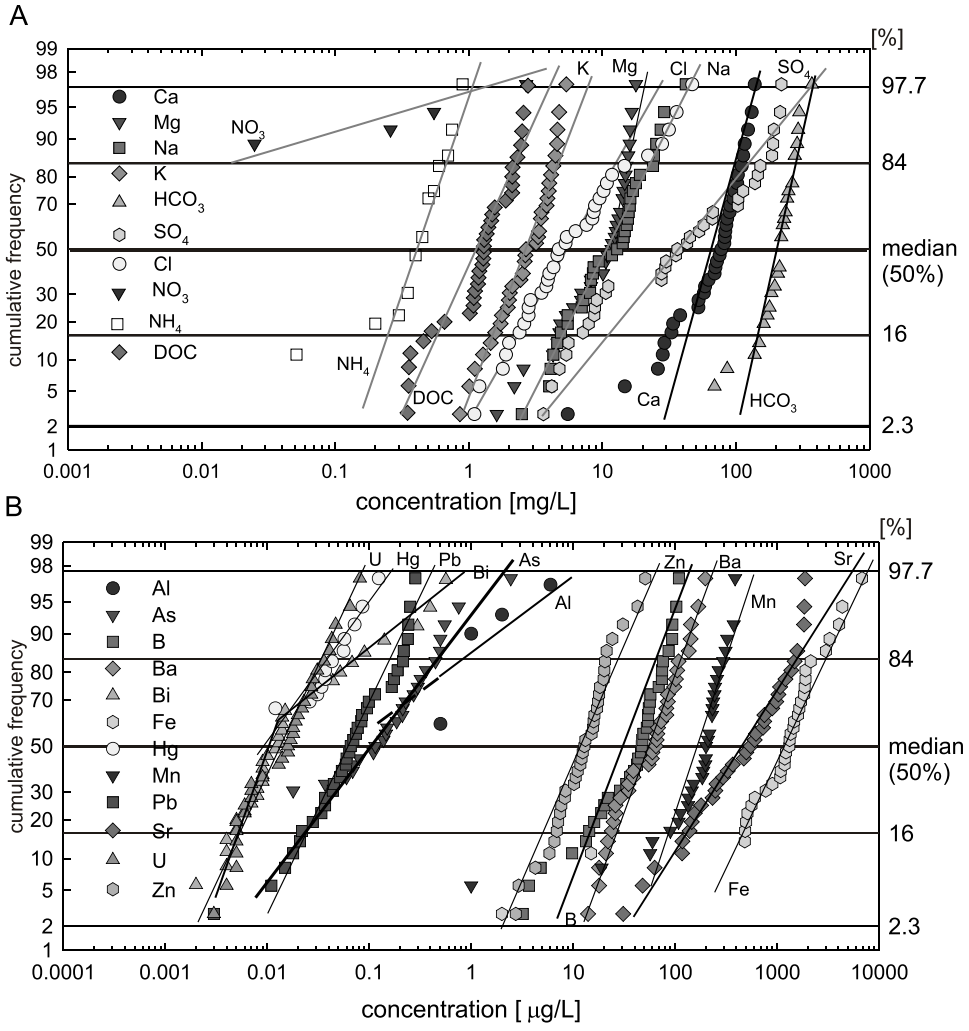

Fig. 13. Cumulative frequency diagrams

A — major and minor components (for a better visualization Sr, Fe and Mn are shown in part b); B — trace components

shown in Figure 12. In general, long travel times through the leaky layers mean that in the confined areas no anthropogenic pollutants should be expected in the near future, except in areas of hydrogeological windows. Similarly, changes in natural influences should be slow and barely observable in the near future.

HYDROCHEMISTRY

Concentrations of major, minor and trace components in waters of the Sarmatian deposits and the buried valleys are shown in the form of cumulative distributions in Figure 13 and as box-plots in Figure 14, whereas the summary statistics are given in Table 2, with the uncertainties related to the last one or two digits of the reported values. Results below the detection level are indicated as being half of the detection level. Due to natural processes, the concentrations of Fe, Mn and NH_4 within the confined part of the aquifer exceed the maximum permissible levels (MPL) of EU regulations (see Table 2). A number of toxic elements are present due to natural processes (e.g. As, Be, Cd, Hg, Sb and Pb), though their abundances are low. The distributions are in most cases wide and irregular and it is not always easy to explain their deviations from straight lines seen in Figure 13. The distributions of NO_3^- and SO_4^{2-} are particularly wide, as are those for SO_4^{2-} and Ca^{2+}, and they deviate from straight lines, suggesting different sources for these components. Measurable aerobic conditions were found only in two wells (no. 8 and 9); therefore, the typical changes in hydrochemistry caused by change in redox conditions along flow lines from recharge areas to confined zones are not visible. No trends in hydrochemistry were observed in wells abstracting ancient water. For wells abstracting modern waters, as indicated by the presence of tritium, no time series of data are available for the previous decades, whereas present observations do not exhibit any clear trends so far.

Artesian water of the Na-Cl-SO_4-HCO_3 type with TDS contents of about 2 700 mg/L occurs in the Triassic deposits in

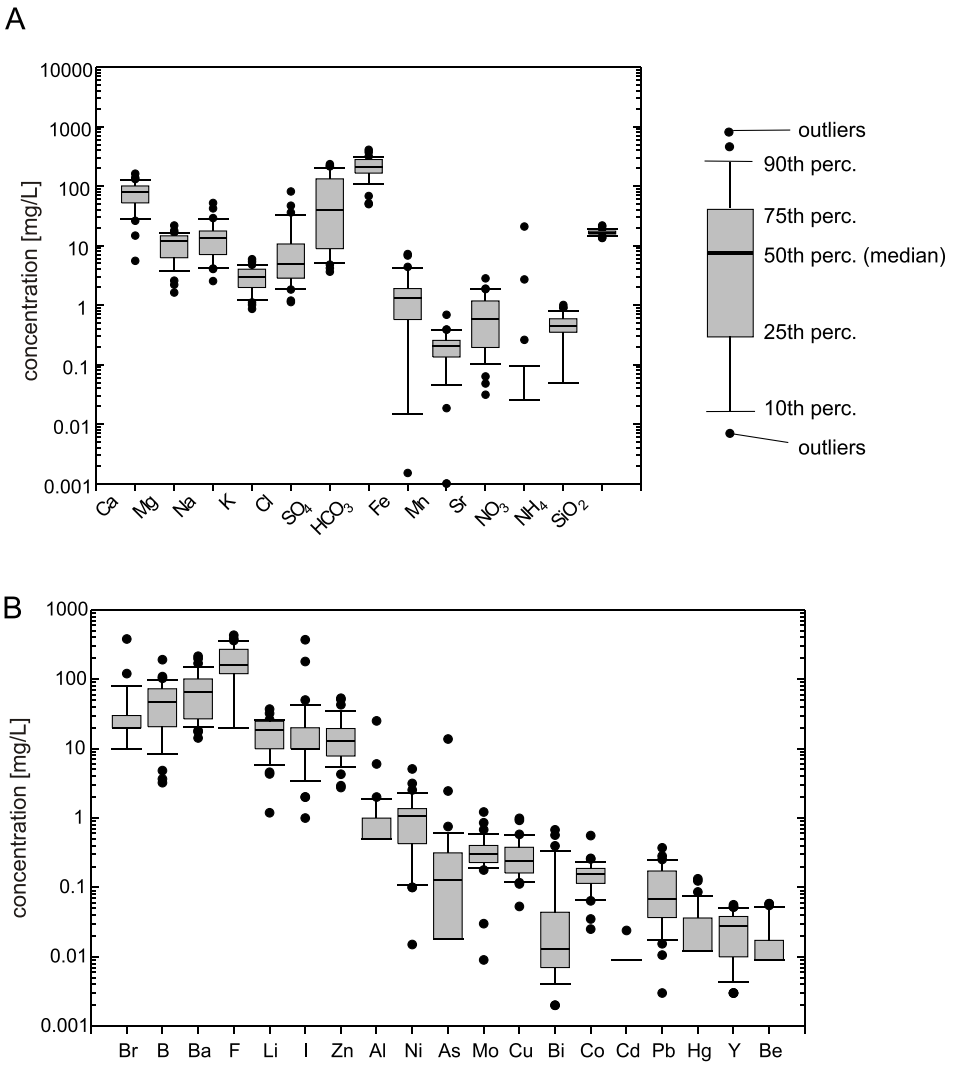

Fig. 14. Box-plots

A — major and minor components, B — trace components

Table 2

Summary statistics

Parameter	Mean	Median	Minimum	Maximum	S.D.	MPL	**2.3%**	**97.7%**
parameters								
T [°C]	12.0	12	9.5	16.2	1.3		9.5	15.6
pH	7.25	7.25	6.29	7.80	0.33	6.5–9.5	6.36	7.79
Eh [mV]	79.2	53.7	-46.3	411	110		–31	393
DO [mg/L]	1.25	0.02	0.00	5.87	1.1		0.00	3.49
SEC [μScm^{-1}]	509	549	125	1063	207		135	861
major and minor components								
Ca [mg/L]	76.2	79.6	5.5	161.0	36.3		12.9	142.5
Mg [mg/L]	10.8	11.8	1.62	21.7	5.0		2.1	18.6
Na [mg/L]	14.6	13.6	2.5	52.0	11	200	3.7	44.0
K [mg/L]	3.02	2.94	0.86	5.91	1.3		0.98	5.48
Cl [mg/L]	11.3	5.0	1.1	80.8	15.9	250	1.2	53.5
SO_4 [mg/L]	72.1	39.7	3.6	233.5	74.0	250	4.1	221.8
HCO_3 [mg/L]	217	209	50	406	80		51	377
Fe [mg/L]	**1.70**	1.33	0.02	**7.19**	1.66	0.20	0.02	**6.88**
Mn [mg/L]	**0.21**	0.21	0.00	**0.69**	0.13	0.10	0.00	**0.45**
Sr [mg/L]	0.77	0.58	0.03	2.81	0.68		0.04	2.06
NO_3 [mg/L]	0.68	0.26	0.02	20.8	3.5	50	0.025	6.22
NH_4 [mg/L]	0.45	0.45	0.05	**1.00**	0.24	0.50	0.05	**0.92**
SiO_2 [mg/L]	16.8	16.6	13.4	21.7	1.8		13.5	21.1
selected trace components								
Br [mg/L]	0.037	0.020	0.005	0.375	0.063		0.006	0.172
B [mg/L]	0.051	0.048	0.003	0.191	0.038	1.0	0.004	0.125
Ba [mg/L]	0.073	0.065	0.014	0.214	0.052		0.017	0.201
F [mg/L]	0.212	0.182	0.053	0.430	0.100	1.5	0.064	0.399
toLi [mg/L]	17.4	18.7	1.2	37.0	8.6		3.7	33.1
I [mg/L]	27.1	7.5	1.0	374	66.8		1.8	219
Zn [mg/L]	16.1	13.0	2.7	53.0	11.9		2.9	51.4
Al [mg/L]	1.70	0.50	0.50	25.00	4.52		0.50	12.33
Ni [mg/L]	1.18	1.10	0.02	5.09	0.98	20.0	0.09	3.61
As [mg/L]	0.62	0.13	0.02	13.70	2.28	10.0	0.02	4.64
Mo [mg/L]	0.36	0.30	0.01	1.22	0.22		0.03	0.92
Cu [mg/L]	0.30	0.24	0.01	0.99	0.22	2000	0.044	0.94
Bi [mg/L]	0.074	0.013	0.002	0.674	0.160		0.002	0.590
Co [mg/L]	0.16	0.16	0.03	0.56	0.09		0.03	0.32
Cd [mg/L]	0.009	0.009	0.009	0.024	0.003	5.0	0.009	0.012
Pb [mg/L]	0.10	0.07	0.003	0.37	0.09	10.0	0.009	0.30
Hg [mg/L]	0.028	0.012	0.012	0.133	0.031	1.0	0.012	0.126
Y [mg/L]	0.027	0.027	0.003	0.056	0.016		0.003	0.053
Be [mg/L]	0.017	0.009	0.009	0.058	0.016		0.009	0.058

MPL — maximum permissible level according to Council Directive 98/83/EC; S.D. — standard deviation of the distribution; 2.3%, 97.7% — percentages of the distribution; (values exceeding the MPL are indicated in bold)

the centre of the basin at depths of 515–550 m (well no. 41). Similar water, though with about 30% lower a TDS content, occurs in well no. 40. Both waters are of glacial age (see Table 1). When well 41 was drilled, artesian water of the Na-SO_4-Cl type with TDS content of about 10 000 mg/L was found at depths of 402–420 m in the Miocene Kłodnica Beds showing a strong hydrochemical inversion (Alexandrowicz and Kleczkowski, 1970). Thermal inversion was also observed as temperatures were 14 and 22°C in the lower and upper levels, respectively. These hydrochemical and thermal inversions

occur only in the area of a deep structure (see Figs. 1 and 2) where the upward seepage is locally hindered by a large thickness of semi-permeable deposits. As a consequence, older water may still be preserved in a less active zone.

The Piper diagram is shown in Figure 15 with arrows indicating possible evolution along flow lines or mixing trends. Judging from that figure, there is no chemical evidence of the distinct natural influence of ascending water on the chemistry of waters in the Sarmatian and buried valley deposits because there are no waters having clear intermediate positions. Therefore, though artesian pressures and tracer data indicate such seepage, its quantitative contribution to the water balance of the Sarmatian aquifer is probably negligible and, consequently, was disregarded in the flow modelling.

The natural hydrochemical evolutions suggested in Figure 15 are probably masked by admixtures of polluted waters at the north-west boundary and influences of ascending waters from the Badenian strata, which take place mainly in the central part of the area.

Water in the Sarmatian aquifer is generally of the HCO_3-Ca type with a TDS content of 250–300 mg/L. In the central part, water changes to the SO_4-Ca type, which confirms an admixture of ascending water from the Badenian deposits where TDS contents are elevated in the central part, being in the range of about 530 to more than 1000 mg/L, with SO_4^{2-} contents of 180 to 400 mg/L. Without the contribution of ascending water from the Badenian deposits, the change in the Sarmatian aquifer would be to the HCO_3-Na type. The hydrochemical influence of downward seepage of modern polluted waters to the Sarmatian aquifer at the centre of the basin is excluded by tracer data and long travel times of downward seepage.

Waters in the Pleistocene buried valley are fresh and due to their relatively old ages they are of HCO_3-Na type. The persistence of that type and generally low SO_4^{2-} contents practically exclude any significant influence of ascension, confirming the conclusion drawn from the hydrochemical inversion found in well 41 that ascension from deeper formations is locally hindered in the deep structure of the Odra buried valley (ascension takes place mainly on the sides of that valley).

The horizontal distributions of Ca^{2+} and SO_4^{2-} obtained by kriging (Englund and Sparks, 1991) are shown in Figures 16 and 17, respectively. The similarity of both figures suggests the origin of Ca^{2+} and SO_4^{2-} to be predominantly related to leaching of gypsum, though the cumulative distributions of both components are very irregular, which means that other sources may also exist. If the area of the study is divided into three regions as shown in Figure 18, the cumulative distributions of SO_4^{2-} for particular regions are more linear and distinctly differ as shown in Figure 19, indicating three different natural background values of SO_4^{2-}. Zone A corresponds to the main buried Pleistocene valley. In spite of old water ages in that zone, the natural SO_4^{2-} contents are very low (4–10 mg/L), with one exception (no. 6), which probably results from the local influence of upward seepage. One well (no. 18) in that zone contains a slightly ele-

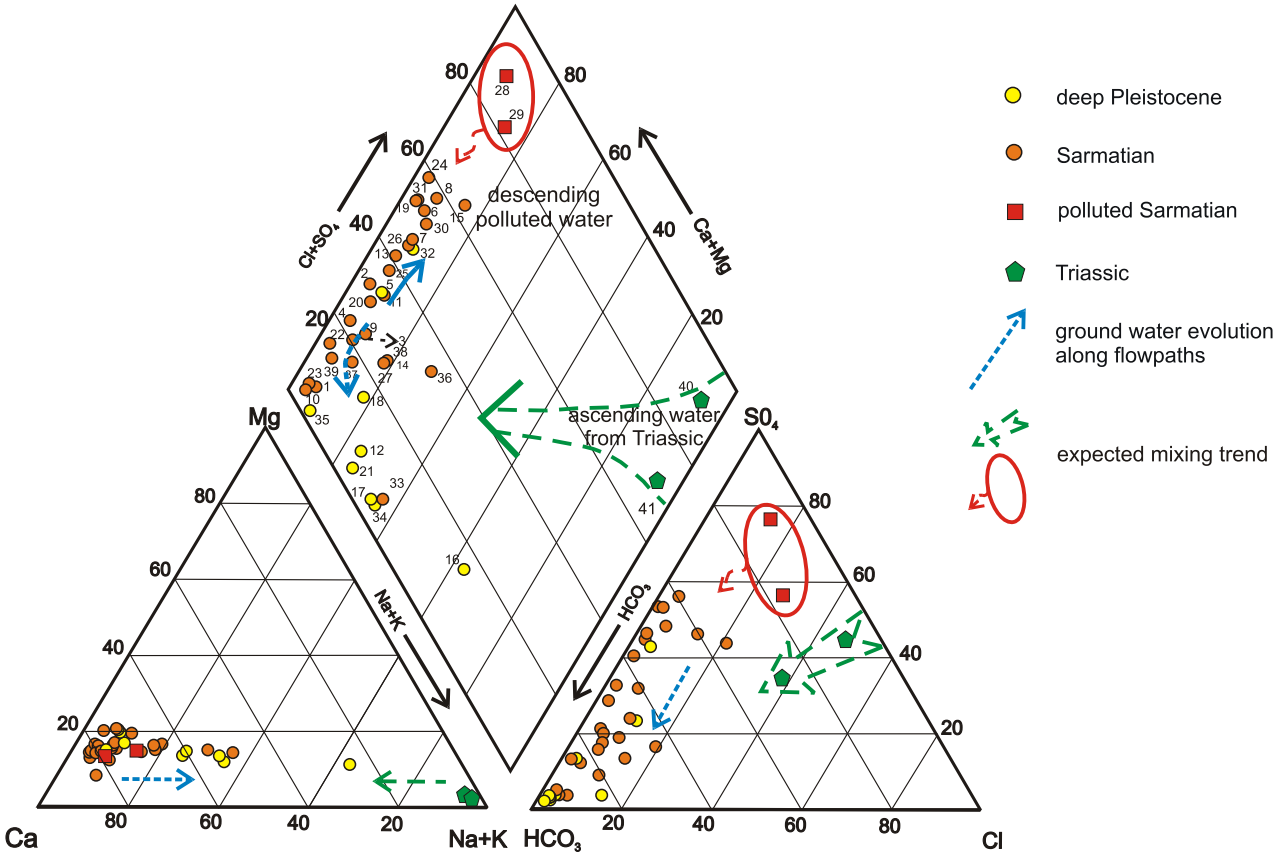

Fig. 15. Tri-linear plot with indicated ground water evolution along flow paths and supposed mixing

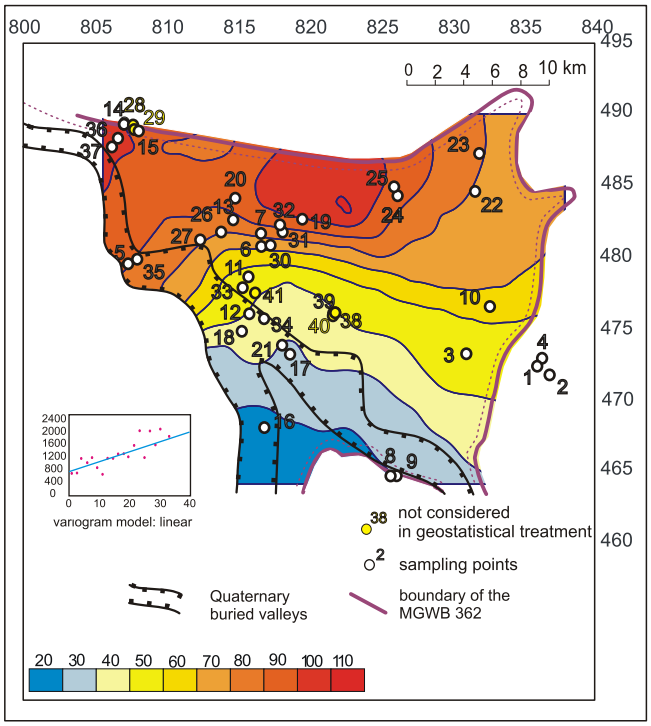

Fig. 16. Kriging map of Ca^{2+} [mg/L] in the NE region of MGWB-332

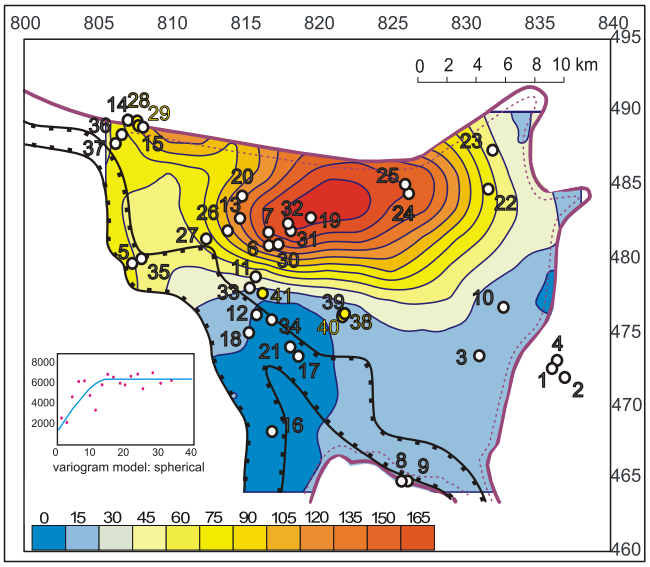

Fig. 17. Kriging map of SO_4^{2-} [mg/L] in the NE region of MGWB-332

For other explanations see Figure 16

vated Cl-content. The SO_4^{2-} concentrations in zone B cover are in the range of 5–50 mg/L. In the eastern part, in spite of intensive recharge by downward seepage, the concentrations from the supposed atmospheric deposition are low. Elevated values are observed in the western part. These elevated values most probably result from an admixture of ascending water from the Badenian deposits. Zone C is the area with the highest natural SO_4^{2-} concentrations (30–200 mg/L) due to the ascension from

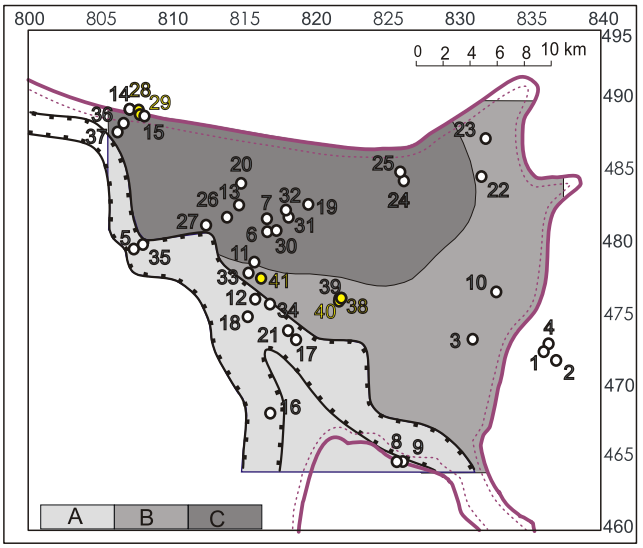

Fig. 18. Three subregions of SO_4^{2-} contents in MGWB-332

A — 4–10 mg/L, B — 5–50 mg/L, C — 30–200 mg/L; for other explanations see Figure 16

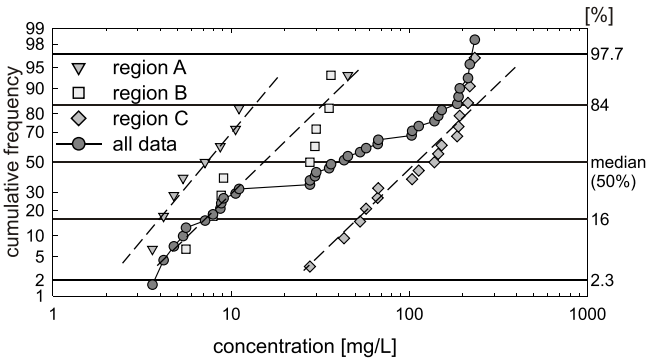

Fig. 19. Cumulative frequencies of SO_4^{2-} for the whole area investigated, and for three subregions with concentration ranges as in Figure 18

the Badenian levels and perhaps a lateral inflow from the Triassic formations at the northern boundary. The highest SO_4^{2-} concentrations, accompanied by elevated Cl-concentrations, are observed in the north-west due to anthropogenic pollution. For instance, waters in wells no. 14 and 15, with SO_4^{2-} concentrations up to 120 mg/L, may be polluted as deduced from their modern origin as determined by tritium data. Modern waters also enter the aquifer close to that area through a small erosion window between the Pleistocene and Sarmatian aquifers (wells 28 and 29). They have very high SO_4^{2-} and relatively high Cl^- concentrations (230 and 300 mg/L, respectively) resulting from leaching of fly-ash disposal sites. Their modern ages are confirmed by tritium data from well no. 28 (see Table 2) whereas well no. 29 was not sampled for tracers. The hydrochemical data of these two wells were not used in the statistical treatment. All the sampled wells in the north-west region have elevated Cl^- contents, which may result from a natural influence because waters in wells 36 and 37 are tritium-free.

CONCLUSIONS

Wide natural distributions of chemical constituents are observed in the Sarmatian aquifer intersected by buried Pleistocene valleys. They can be regarded as typical of the majority of confined aquifers, which means that a representative determination of natural background levels (NBL), required by EU Directives, can be difficult or even impossible on the basis of samples taken from a low number of sites (wells). In such cases, the estimation of the quality of water even for a GWB representing a homogeneous aquifer can also be of doubtful value.

Representativeness of the NBL by a single value (e.g. by 97.7 percentile or any other chosen value) is questionable. Therefore, the range of 2.3 to 97 percentiles of the cumulative concentration distributions can be suggested as a more representative choice for the presentation of NBL values of ground water constituents. The additional advantage of such presentation is that the standard deviation (S.D.) of the natural distribution is easily obtainable as the proposed range corresponds roughly to 4 S.D. (± 2 S.D.).

The problem of a representative presentation of NBL becomes even more difficult if different hydrochemical zones exist as is shown for SO_4^{2-} in the case of the Sarmatian deposits and Pleistocene buried valleys of GWB-129. Although other aquifers of that GWB were not investigated within the present work, there is no doubt that, if they were included, the observed distributions would be much wider and an adequate presentation of NBLs more difficult.

For GWB-129 and other similar multi-aquifer GWBs, ground water dependent ecosystems can be influenced only by the shallow aquifer(s) whereas confined aquifer(s) are of great importance for human receptors as a source of drinking water. In such cases, it may be very difficult to define uniquely the chemical status of the entire GWB. Therefore, it seems that a distinction should be introduced between the shallow and deeper parts of multi-aquifer GWBs.

Predictions of quality changes in some multi-aquifer GWBs, also those caused by conservative pollutants and/or natural influences may be difficult or even impossible because travel times of seepages through aquitards are distinctly larger than possible observation periods. For the central parts of the Sarmatian deposits and Pleistocene buried valleys of GWB-129, tracer data and numerical modelling of flow and transport yielded ages of the order of thousands years. Therefore, it is not surprising that no trends in hydrochemistry were observed.

Acknowledgements. This work was partly supported by statutory funds of the AGH University of Science and Technology (projects nos. 11.11.220.01 and 11.11.140.139).

REFERENCES

ALEXANDROWICZ S. W. and KLECZKOWSKI A. S. (1968) — The tectonics of the Triassic in the western margin of the Upper Silesian Coal Basin. Bull. Acad. Pol. Sc., Sér. Sc. Géol. Géogr., **16** (3–4): 171–176.

ALEXANDROWICZ S. W. and KLECZKOWSKI A. S. (1970) — Le profil stratigraphique et les eaux minérale du forage de Kedzierzyn. Bull. Acad. Pol. Sc., Sér. Sc. Géol. Géogr., **18** (4): 199–207.

BUSENBERG E. and PLUMMER L. N. (2000) — Dating young groundwater with sulfur hexafluoride: natural and anthropogenic sources of sulfur hexafluoride. Water Resour. Res., **36**: 3011–3030.

CLARK I. and FRITZ P. (1997) — Environmental Isotopes in Hydrogeology. Lewis Publ. New York.

COPLEN T. B. (1996) — New guidelines for reporting stable hydrogen, carbon and oxygen isotope-ratio data. Geochim. Cosmochim. Acta, **60**: 3359–3360.

d'OBYRN K., GRABCZAK J. and ZUBER A. (1997) — Maps of isotopic composition of the Holocene meteoric waters in Poland (in Polish with English summary). Współczesne problemy hydrogeologii (ed. J. Górski and E. Liszkowska): 331–333. VIII Symp. Kierz k/Poznania. Wind, Wrocław.

DULIŃSKI M., KMIECIK E., OPOKA M., RÓŻAŃSKI K., SZCZAPAŃSKA J., SZKLARCZYK T., ŚLIWKA I., WITCZAK S. and ZUBER A. (2002) — Hydrochemistry of Kędzierzyn Subtrough aquifer as related to water ages. Jakość i podatność wód podziemnych na zanieczyszczenie. Prace Wydz. Nauk o Ziemi Uniw. Śląskiego, **22**: 35–43.

EDMUNDS W. M. and SHAND P. eds. (2007) — The Natural Baseline Quality of Groundwater. Blackwell Publ. (in press).

ENGLUND E. and SPARKS A. (1991) — Geostatistical environmental assessment software. User's guide. U.S. Environ. Protect. Agency, Nevada EPA/600/8-91/008.

EUROPEAN UNION DIRECTIVES (1998) — Council Directive 98/83/EC of 3 November 1998 on the quality of water intended for human consumption. Official Journal L 330, 05/12/1998: 0032–0054.

EUROPEAN UNION DIRECTIVES (2000) — Directive 2000/60/EC of the European Parliament and of the Council of 23 October 2000 establishing a framework for Community action in the field of water policy. Official Journal L 327, 22/12/2000: 0001–0073.

EUROPEAN UNION DIRECTIVES (2006) — Groundwater Daughter Directive — Proposal for a Directive of the European Parliament and of the council on the protection of groundwater against pollution (COM(2003)550), 23 January 2006.

GUIGER N. and FRANZ T. (2003) — Visual MODFLOW Pro v.3.1.Waterloo Hydrol. Inc.

HERBICH P., HORDEJUK T., KAZIMIERSKI B., NOWICKI Z., SADURSKI A. and SKRZYPCZYK L. (2005) — Groundwater bodies in Poland (in Polish). Współczesne problemy hydrogeologii, T. XII (eds. A. Sadurski and A. Krawiec): 269–274. Wyd. Uniw. Mikołaja Kopernika, Toruń.

KLECZKOWSKI A. S. (1966) — Subquaternary substratum of the upper Odra basin and its water-bearing layers (in Polish with English summary). Prace Geol. PAN, Kraków.

KLECZKOWSKI A. S. *et al*. (1990) — The map of the critical protection areas (CPA) of the Major Groundwater Basins (MGWB) in Poland. Acad. Min. Metal. Kraków.

KOTLICKA G. N. (1975) — The Quaternary of the vicinity of Kotlarnia, west of Gliwice (in Polish with English summary). Biul. Inst. Geol. 282: 475–521.

KOTLICKA G. N. (1978) — Stratigraphy of the Quaternary in the Odra Valley near Racibórz (in Polish with English summary). Biul. Inst. Geol., **300**: 303–387.

KOTLICKA G. N. (1981) — Neotectonics of the Upper Odra Valley (in Polish with English summary). Biul. Inst. Geol., **321**: 165–175.

MAŁOSZEWSKI P. and ZUBER A. (1996) — Lumped parameter models for the interpretation of environmental tracer data. Manual on Mathematical Models in Isotope Hydrology. IAEA-TECDOC-910, IAEA, Vienna: 9–58.

McDONALD M. G. and HARBOUGH A.W. (1988) — MODFLOW, A modular three-dimensional finite difference ground-water flow model. U.S. Geol. Surv. Open-file Rep.: 83–875. Unit. Stat. Geol. Surv.

POLLOCK D. W. (1988) — Semianalytical computation of path lines for finite difference models. Ground Water, **26**: 743–750.

SANFORD W. E. (1997) — Correcting for diffusion in carbon-14 dating of ground water. Ground Water, **35** (2): 357–361.

SALMINEN R. ed. (2005) — Geochemical Atlas of Europe. Part 1. Background Information, Methodology and Maps. Geol. Surv. Finland. Espoo.

SUDICKY E. A. and FRIND E. O. (1981) — Carbon-14 dating of groundwater in confined aquifers: implications of aquitard diffusion. Wat. Resour. Res., **17**: 1060–1064.

SZCZEPAŃSKA J. and KMIECIK E. (2005) — Ocena stanu chemicznego wód podziemnych w oparciu o wyniki badań monitoringowych. Wyd. AGH Univ. Sc. Technol., Kraków.

SZKLARCZYK T., WITCZAK S. and NAŁĘCKI P. (2004) — Hydrogeological model of the Kędzierzyn-Głubczyce subtrough (MGBW 332) as an example of a complex groundwater system simulation (in Polish). Modelowanie przepływu wód podziemnych (ed. J. Gurwin and S. Staśko). Acta Univ. Wratislav., **2729**: 253–269.

ŚLIWKA I., LASA J., ZUBER A., OPOKA M. and JACKOWICZ-KORCZYŃSKI M. (2004) — Headspace extraction method for simultaneous determination of SF_6, $CC_{l3}F$, $CC_{l2}F_2$ and $CC_{l2}FCC_lF_2$ in water. Chem. Anal., **49**: 535–549.

ZHENG C. and WANG P. P. (1999) — *MT3DMS*, A modular three-dimensional multi-species transport model for simulation of advection, dispersion and chemical reactions of contaminants in groundwater systems; documentation and user's guide. U.S. Army Eng. Res. Develop. Center Contract Rep. SERDP-99-1, Vicksburg, Mississippi.

ZUBER A., WITCZAK S., RÓŻAŃSKI K., ŚLIWKA I., OPOKA M., MOCHALSKI P., KUC T., KARLIKOWSKA J., KANIA J., JACKOWICZ-KORCZYŃSKI M. and DULIŃSKI M. (2005) — Groundwater dating with ^3H and SF_6 in relation to mixing pattern, transport modeling and hydrochemistry. Hydrol. Proc., **19**: 2247–2275.